



AALBORG UNIVERSITY
DENMARK

Aalborg Universitet

Interharmonics Reduction in Photovoltaic Systems with Random Sampling MPPT Technique

Sangwongwanich, Ariya; Blaabjerg, Frede

Published in:

Proceedings of the IEEE Energy Conversion Congress and Exposition (ECCE 2019)

DOI (link to publication from Publisher):

[10.1109/ECCE.2019.8912741](https://doi.org/10.1109/ECCE.2019.8912741)

Publication date:

2019

Document Version

Early version, also known as pre-print

[Link to publication from Aalborg University](#)

Citation for published version (APA):

Sangwongwanich, A., & Blaabjerg, F. (2019). Interharmonics Reduction in Photovoltaic Systems with Random Sampling MPPT Technique. In *Proceedings of the IEEE Energy Conversion Congress and Exposition (ECCE 2019)* (pp. 4760-4765). Article 8912741 IEEE Press. <https://doi.org/10.1109/ECCE.2019.8912741>

General rights

Copyright and moral rights for the publications made accessible in the public portal are retained by the authors and/or other copyright owners and it is a condition of accessing publications that users recognise and abide by the legal requirements associated with these rights.

- Users may download and print one copy of any publication from the public portal for the purpose of private study or research.
- You may not further distribute the material or use it for any profit-making activity or commercial gain
- You may freely distribute the URL identifying the publication in the public portal -

Take down policy

If you believe that this document breaches copyright please contact us at vbn@aub.aau.dk providing details, and we will remove access to the work immediately and investigate your claim.

Interharmonics Reduction in Photovoltaic Systems with Random Sampling MPPT Technique

Ariya Sangwongwanich and Frede Blaabjerg

Department of Energy Technology, Aalborg University, Aalborg DK-9220, Denmark

ars@et.aau.dk, fbl@et.aau.dk

Abstract—An increasing penetration level of grid-connected Photovoltaic (PV) systems raises a concern regarding power quality problem, in particularly, interharmonics. According to previous research, the perturbation from the Maximum Power Point Tracking (MPPT) algorithm is one of the main root-cause of interharmonic emission in PV systems. In general, the interharmonic characteristics are strongly dependent on the sampling rate of the MPPT algorithm. A slow sampling rate of the MPPT algorithm can minimize the interharmonic emission but it results in poor tracking performance of the MPPT algorithm. Thus, there is a trade-off between the interharmonic emission and the MPPT efficiency when selecting the MPPT sampling rate. To overcome this problem, a new MPPT technique implemented with a random sampling rate is proposed in this paper. The proposed method randomly selects the MPPT algorithm sampling rate during each perturbation. This method is simple to be implemented but results in a significant reduction in the interharmonics of the output current and, at the same time, a high MPPT efficiency. The effectiveness of the proposed method has been validated experimentally with a single-phase grid-connected PV system. Moreover, the effect of interharmonic cancellation when implementing the proposed random sampling MPPT technique with parallel-connected PV inverters has also been demonstrated.

Index Terms—Photovoltaic (PV) systems, inverters, maximum power point tracking (MPPT), interharmonics, power quality.

I. INTRODUCTION

During the last decade, an accelerated penetration level of Photovoltaic (PV) system has risen challenging issues regarding grid integration. Among others, power quality problems have been increasingly concerned recently, especially regarding harmonics and interharmonics [1]. Recent studies have indicated that one emerging power quality problem for grid-connected PV systems is related to the interharmonics [2]. By definition, the interharmonics are the frequency components that are non-integer times of the fundamental frequency [3], as illustrated in Fig. 1. Several laboratory testing results from commercial PV inverters have shown that PV systems can be a potential source of interharmonic emission [4]–[7]. The results agree well with the field measurement in [8], where the interharmonics have been observed from the PV systems installed in Sweden. Since the interharmonics can potentially cause grid voltage fluctuations, flickering, and disconnection of PV systems, mitigating solutions are needed.

It was suggested by the previous observation that the Maximum Power Point Tracking (MPPT) control is the one main root cause of the interharmonics from PV inverters. More specifically, most of the MPPT algorithms (e.g., the perturb

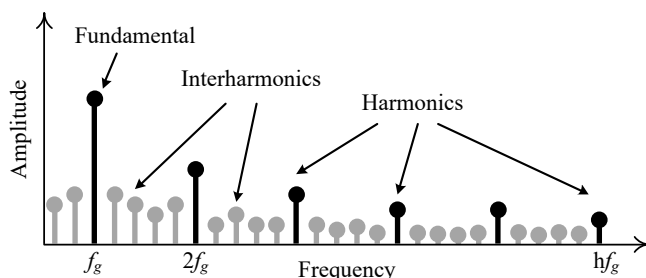


Fig. 1. Definition of harmonics and interharmonics according to the frequency domain representation.

and observe method) intentionally perturbs the operating point of the PV array (e.g., PV voltage) during the Maximum Power Point (MPP) searching, as it is illustrated in Fig. 2. For these algorithms, the power oscillation during the steady-state cannot be avoided where the operating point of the PV system will oscillate around the MPP (e.g., between b , c , and d) [9]. Since the perturbation is periodically applied according to the sampling rate of the MPPT algorithm, it will inevitably cause power oscillations at the dc side, which can then be propagated to the ac side and appearing as interharmonics in the output current. The behavior of interharmonics in PV systems has been analyzed and explained with the model given in [10].

Due to the fact that the interharmonics are driven by the MPPT perturbation, the MPPT algorithm parameters such as its sampling rate will inevitably have a strong impact on the interharmonic characteristics in terms of frequency component but also the amplitude. In general, employing a fast sampling rate for MPPT algorithm can induce significant interharmonics in the output current of the PV inverter. Thus, a slow sampling rate is recommended in order to reduce the interharmonic emission [10]. However, using a slow sampling rate will inevitably reduce the tracking speed and thus the efficiency of the MPPT algorithm [11]. This can result in a considerable amount of loss in the energy yield especially during the dynamic conditions (e.g., changing solar irradiance condition) [12]. Therefore, in the conventional MPPT implementation (i.e., fixed sampling rate), there is a trade-off between the interharmonic emission and the MPPT efficiency when selecting the sampling rate of the MPPT algorithm.

With the above motivation, a new method to mitigate the interharmonics while maintaining a high MPPT performance

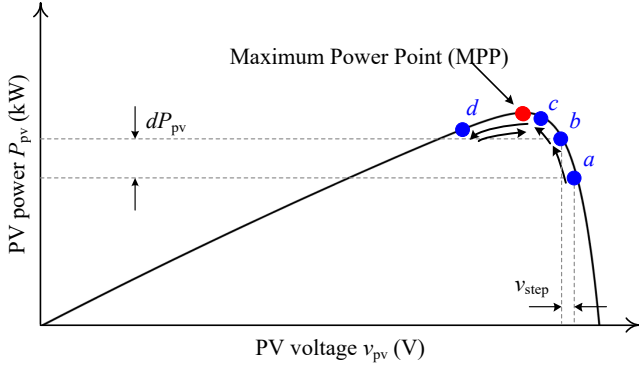


Fig. 2. Operating principle of Perturb and Observe (P&O) maximum power point tracking algorithm in a PV system.

is demanded. Since the characteristics of the interharmonics are dictated by the sampling rate of the MPPT algorithm, modifying the sampling rate of the MPPT algorithm during the operation is one possible solution to achieve the above requirement. Instead of applying a fixed sampling rate for the MPPT algorithm, which has the limitation as discussed above, the sampling rate of the MPPT algorithm can be randomly selected either at a fast or slow value during the operation [13]. By doing so, the perturbation from the MPPT algorithm will be more arbitrary, and the interharmonic emission can be reduced due to the distribution of the frequency spectrum. On the other hand, the MPPT performance can be maintained close to that of the operation with a fast sampling rate of the MPPT algorithm due to the switching operation between the fast and the slow sampling rate. The random sampling technique has previously been applied in Pulse-Width Modulation (PWM) for switching harmonic reduction [14]. However, its application in the MPPT-based algorithm is yet to be explored and validated, especially in terms of interharmonic mitigation. Moreover, the previous study only focuses on the operation of a single PV inverter while the possibility for interharmonics cancellation with parallel operation of PV inverters, e.g., large-scale PV systems, has not been explored.

In this paper, a random sampling MPPT technique is proposed. The MPPT-driven interharmonics in grid-connected PV systems is briefly demonstrated in Section II. Then, in Section III, the implementation of the proposed method is discussed and its performance is validated experimentally. Furthermore, an implementation of the proposed method with parallel-connected PV inverters has also been demonstrated in Section IV, where the stochastic behavior of MPPT perturbation can enhance the effectiveness of interharmonic reduction. Finally, concluding remarks are provided in Section V.

II. INTERHARMONICS IN GRID-CONNECTED PHOTOVOLTAIC SYSTEMS

A. System Configuration

A single-phase grid-connected PV system as shown in Fig. 3 is considered in this paper. This system configuration is also

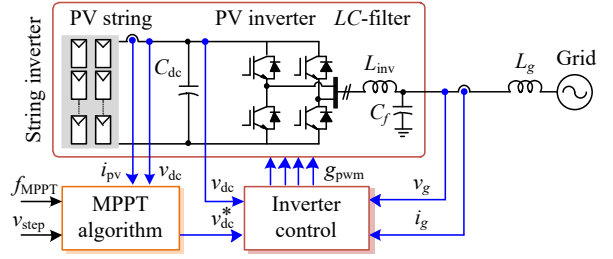


Fig. 3. System diagram of a single-phase PV system with string inverter topology operating with Maximum Power Point Tracking (MPPT) algorithm.

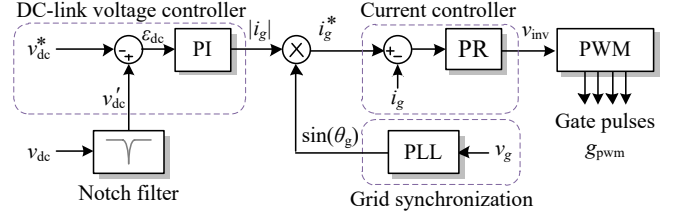


Fig. 4. Control diagram of single-phase grid-connected PV inverter.

TABLE I
PARAMETERS OF THE SINGLE-PHASE GRID-CONNECTED PV SYSTEM.

PV rated power	3 kW
DC-link capacitor	$C_{dc} = 1100 \mu\text{F}$
LC-filter	$L_{inv} = 4.8 \text{ mH}$, $C_f = 4.3 \mu\text{F}$
Grid-side inductance	$L_g = 2 \text{ mH}$
Switching frequency	$f_{inv} = 8 \text{ kHz}$
Controller sampling frequency	$f_s = 20 \text{ kHz}$
Grid nominal voltage (RMS)	$V_g = 230 \text{ V}$
Grid nominal frequency	$f_g = 50 \text{ Hz}$

known as a string inverter topology, where each PV string (a series connection of PV arrays) is equipped with a PV inverter [15]. The inverter is responsible to control the power extraction from the PV string where the MPPT control is implemented. This is normally achieved by regulating the operating voltage of the PV arrays, i.e., the dc-link voltage, to be at the MPP during the operation, in order to maximize the energy yield.

The overall control diagram of the single-phase PV inverter is shown in Fig. 4. The dc-link voltage is regulated through the Proportional-Integral (PI) controller, which determines the corresponding amplitude of output current $|i_g|$. Then, by multiplying the amplitude of output current $|i_g|$ with the phase angle $\sin(\theta_g)$, the reference output current i_g^* can be obtained and regulated with the current controller [16].

B. Interharmonics driven by MPPT Operation

The MPPT algorithm implemented in the PV inverter is basically a search algorithm where the Perturb and Observed (P&O) method is one of the most commonly used MPPT algorithm. The P&O MPPT method requires the perturbation of the PV array voltage in order to determine the next operating point based on the change in the PV output power. Unfortunately,

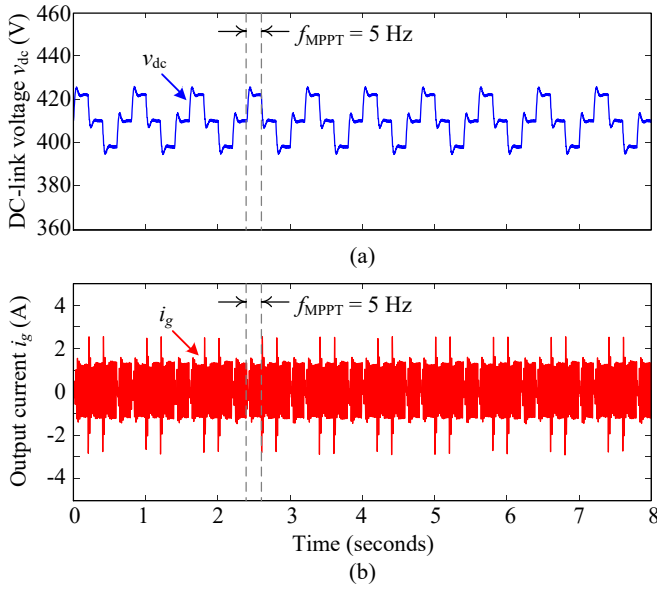


Fig. 5. Experimental waveform of the PV inverter operated at 10 % of the rated power (i.e., 300 W) with the MPPT sampling rate of $f_{MPPT} = 5$ Hz: (a) dc-link voltage v_{dc} and (b) output current i_g .

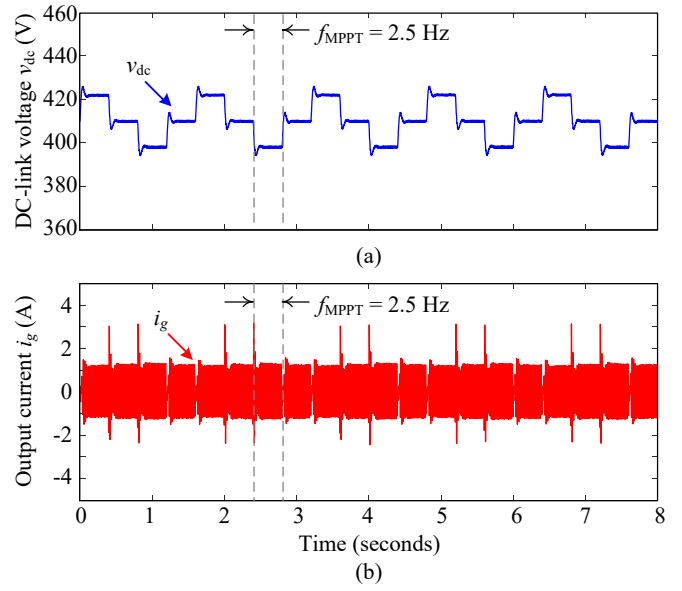


Fig. 7. Experimental waveform of the PV inverter operated at 10 % of the rated power (i.e., 300 W) with the MPPT sampling rate of $f_{MPPT} = 2.5$ Hz: (a) dc-link voltage v_{dc} and (b) output current i_g .

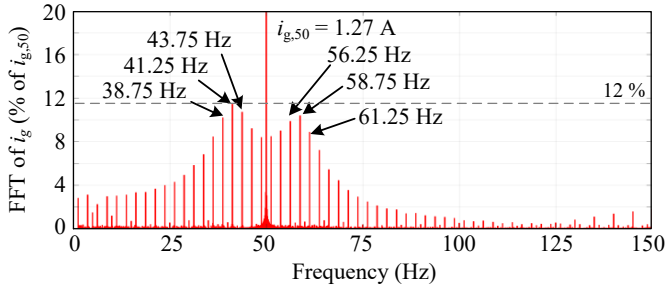


Fig. 6. Frequency spectrum of the output current i_g (in percentage of the 50 Hz component) when the MPPT sampling rate is $f_{MPPT} = 5$ Hz.

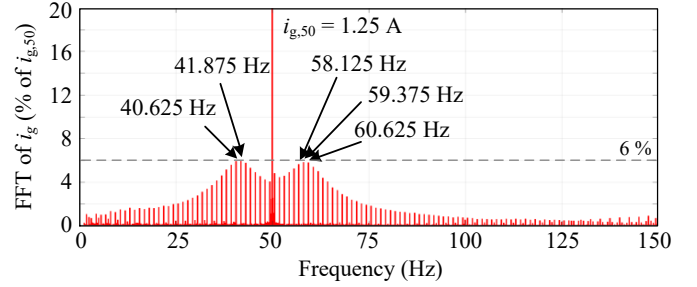


Fig. 8. Frequency spectrum of the output current i_g (in percentage of the 50 Hz component) when the MPPT sampling rate is $f_{MPPT} = 2.5$ Hz.

this perturbation will induce oscillations in the dc-link voltage during steady-state, and thereby the PV output power, as it is demonstrated in Fig. 5(a). The perturbation of the dc-link voltage will inevitably result in an abrupt change in the output current amplitude $|i_g|$ due to the cascaded control structure. Therefore, this oscillation will be propagated to the output current of the inverter i_g through the amplitude modulation between the output current amplitude $|i_g|$ and the phase angle of the grid voltage $\sin(\theta_g)$ following the control diagram in Fig. 4. As a result, the output current of the PV inverter will also experience a periodical perturbation during steady-state, as it is shown in Fig. 5(b). The frequency spectrum of the time-domain waveform of the output current (in Fig. 5(b)) is shown in Fig. 5(c). It can be observed that there are interharmonics, which are concentrated around the fundamental frequency of the output current (e.g., 50 Hz). This interharmonic behavior is correlated with the observation in the previous testing [7] and analysis [8].

C. Impact of MPPT Sampling Rate on the Interharmonics

In the previous case, the interharmonic characteristics under the MPPT sampling rate of $f_{MPPT} = 5$ Hz has been demonstrated in Figs. 5 and 6. In order to demonstrate the impact of MPPT sampling rate on the interharmonics, an operating condition under another MPPT sampling rate is considered for comparison. The time-domain waveform of the operating condition under the MPPT sampling rate of $f_{MPPT} = 2.5$ Hz is shown in Fig. 7. Compared with the case in Fig. 5, it can be seen that the dc-link voltage v_{dc} and the output current i_g in Fig. 7 is less frequently perturbed, corresponding to the applied MPPT sampling rate. The frequency spectrum of the output current when the MPPT sampling rate is $f_{MPPT} = 2.5$ Hz is shown in Fig. 8. It can be seen that the interharmonics in the output current is less pronounced when employing a slow MPPT sampling rate (e.g., $f_{MPPT} = 2.5$ Hz). Therefore, it was recommended to employ a slow MPPT sampling rate for the MPPT algorithm considering the interharmonic emis-

sion. Nevertheless, the MPPT tracking performance may be compromised, especially under a fast changing solar irradiance condition (e.g., due to passing clouds).

III. PROPOSED RANDOM SAMPLING MPPT TECHNIQUE

A. Modifying MPPT Sampling Rate

Conventional P&O MPPT algorithm is implemented with a fixed sampling rate, as it has been demonstrated in the previous section. However, it has a trade-off between interharmonic emission and MPPT efficiency. To address this issue, a novel implementation of MPPT algorithm is required. One possible solution to overcome this limitation is by employing a random sampling rate for the MPPT algorithm. In this method, the MPPT algorithm sampling rate f_{MPPT} is randomly selected after each perturbation either at a fast f_{fast} or a slow f_{slow} value, which can be implemented as

$$f_{MPPT} = \begin{cases} f_{fast}, & \text{when } X \leq 0.5 \\ f_{slow}, & \text{when otherwise} \end{cases} \quad (1)$$

where $X \sim U(0,1)$ is a random variable with uniform distribution between 0 and 1.

An example of the random sampling MPPT operation is demonstrated in Fig. 9(a) where the sampling rates are $f_{fast} = 5$ Hz and $f_{slow} = 2.5$ Hz. It can be seen from the waveform of the dc-link voltage that the perturbation frequency is switched between 5 Hz and 2.5 Hz during the operation in a random manner. Consequently, the perturbation behavior from the MPPT algorithm in Fig. 9(a) will be more arbitrary compared to the case with fixed sampling rate implementation in Figs. 5(a) and 7(a). This random perturbation is also reflected in the waveform of the output current in Fig. 9(b).

B. Interharmonics Reduction

The effectiveness of the proposed random sampling MPPT technique in terms of interharmonics mitigation can be validated by considering the frequency spectrum of the output current. As it can be seen from the results in Fig. 10, the interharmonics can be reduced significantly when applying the random sampling MPPT technique compared to the case with $f_{MPPT} = 5$ Hz in Fig. 6. With the proposed method, the peak amplitude of the interharmonics is reduced from 12 % (i.e., when applying $f_{MPPT} = 5$ Hz) to 6 %. In fact, the interharmonic emission level of the proposed method is similar to that when applying a slow sampling rate of the MPPT algorithm $f_{MPPT} = 2.5$ Hz in Fig. 8, i.e., the peak amplitude of the interharmonics is 6 %. Accordingly, the proposed random sampling MPPT method can effectively reduce the interharmonic emission from the PV systems.

C. MPPT Efficiency

The MPPT efficiency is a performance metric that has a direct impact on the energy yield, and thus has to be evaluated and benchmarked between different methods. The MPPT efficiency η_{MPPT} can be calculated as

$$\eta_{MPPT} = \frac{E_{pv}}{E_{avai}} \quad (2)$$

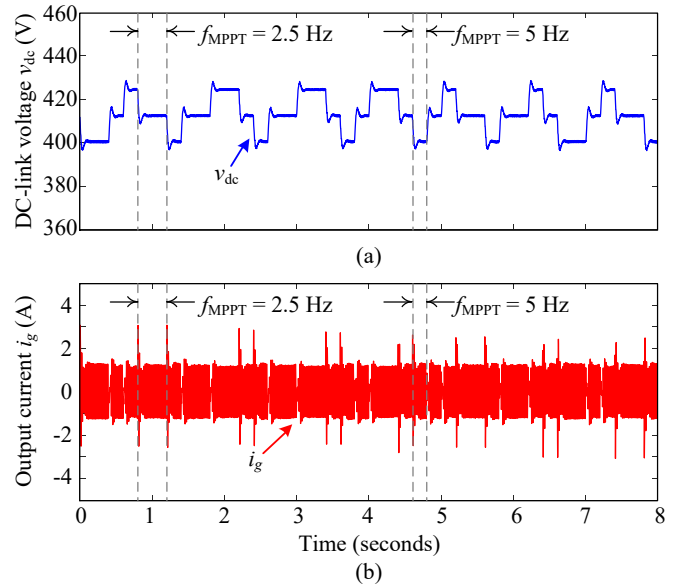


Fig. 9. Experimental waveform of the PV inverter operated at 10 % of the rated power with the proposed random sampling MPPT technique ($f_{fast} = 5$ Hz and $f_{slow} = 2.5$ Hz): (a) dc-link voltage v_{dc} and (b) output current i_g .

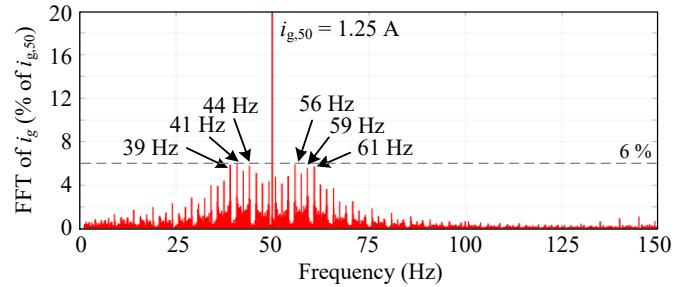


Fig. 10. Frequency spectrum of the output current i_g (in percentage of the 50 Hz component) with the random sampling MPPT technique.

where E_{pv} and E_{avai} are the extracted and available PV energy, respectively. A trapezoidal solar irradiance profile is considered in the experiments since it includes both the dynamic and the steady-state operating conditions. It can be seen from the results in Figs. 11(a) and 11(b) that the MPPT algorithm can follow the change in the available power better when a fast sampling rate is employed (e.g., $f_{MPPT} = 5$ Hz), especially during the changing of solar irradiance condition. This result in 0.5 % higher MPPT efficiency and thus the total energy yield compared to the case with $f_{MPPT} = 2.5$ Hz.

The MPPT performance of the proposed method is also evaluated by using the same operating condition. It can be seen from the result in Fig. 11(c) that the MPPT performance of the proposed method is clearly improved compared to the case with slow MPPT sampling rate in Fig. 11(b). In fact, the combination between the fast and the slow sampling rate used in the proposed method resulted in a similar MPPT efficiency as the case with the fast MPPT sampling rate (e.g., $f_{MPPT} = 5$ Hz), where only 0.01 % reduction in the MPPT efficiency is

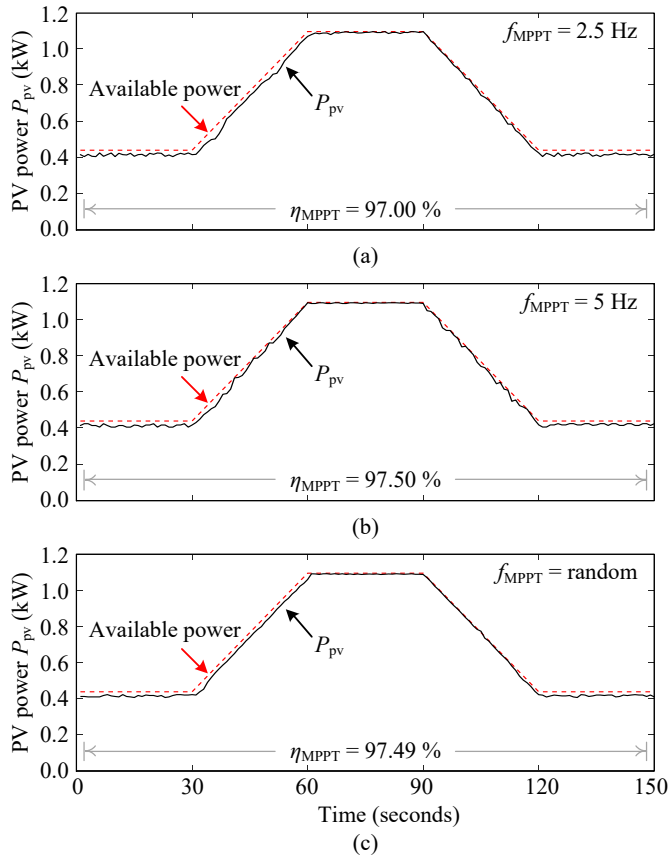


Fig. 11. Measured power extraction of the PV inverter with different MPPT sampling rates: (a) $f_{\text{MPPT}} = 5$ Hz, (b) $f_{\text{MPPT}} = 2.5$ Hz, and (c) $f_{\text{MPPT}} = \text{random}$.

observed. Thus, a high MPPT performance can be ensured with the proposed method while the interharmonics in the output current are reduced considerably.

IV. OPERATION WITH PARALLEL INVERTERS

So far, an operation of a single PV inverter is considered in the analysis. However, in large-scale PV systems, several string inverters can be employed and they are normally connected in parallel in order to increase the power rating. In this section, a possibility to further enhance the effectiveness of the proposed method by means of interharmonic cancellation in parallel-connected PV inverters will be discussed and demonstrated.

A. Parallel-Connected PV Inverters

In this paper, two parallel-connected PV strings shown in Fig. 12 are considered. The system parameters (of each string) are similar to that given in Table I. The total output current at the Point of Common Coupling (PCC) i_g , which is the sum of each string inverter current (i.e., $i_g = i_{g1} + i_{g2}$), is of interest in terms of interharmonics.

When each individual PV string is implemented with the random sampling MPPT operation, the stochastic behavior of perturbation has a high probability to counteract one another. This can potentially smooth out the total power oscillation and

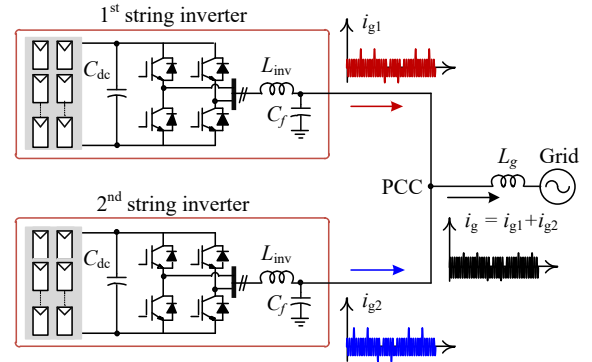


Fig. 12. Operation of two string PV inverters parallel-connected at the Point of Common Coupling (PCC).

thereby further reduce the interharmonics in the total output current. An example of the random sampling MPPT operation with two parallel-connected PV inverters is demonstrated in Fig. 13. The stochastic behavior of the MPPT perturbation of each PV string can be seen from the time-domain waveforms of the dc-link voltage in Fig. 13(a). It can be noticed that in a few occasions the perturbation behavior of the two inverters is counteracting one another. This is also reflected in the perturbation of the output current of each PV string in Fig. 13(b) and (c). Consequently, the perturbation in the total output current shown in Fig. 13(d) is relatively less visible compared to the operation of a single inverter.

B. Interharmonics Reduction

The impact of the parallel operation of PV inverters on the interharmonics reduction can be demonstrated by considering the frequency spectrum of the total output current at the PCC, as it is shown in Fig. 14. Compared with the other cases in Figs. 6, 8, and 10, the parallel operation of PV inverters results in the lowest interharmonic emission with the peak amplitude of the interharmonics of 4%. In other words, the effectiveness of the random sampling MPPT method in terms of interharmonics reduction is further enhanced with the parallel-connected PV inverters, thanks to the stochastic behavior of the perturbation.

V. CONCLUSIONS

In the conventional MPPT technique, there is a trade-off between the interharmonic emission and the MPPT performance when selecting the sampling rate. To overcome this limitation, a new MPPT technique implemented with a random sampling rate is proposed in this paper. The proposed algorithm randomly switches the sampling rate of the MPPT algorithm between a fast and a slow values, which can smooth out a certain amount of power oscillation during the MPP searching. As a result, the interharmonic emission can be significantly reduced. Meanwhile, the tracking performance of the MPPT algorithm is maintained similar to the case with a fast MPPT sampling rate. Further, the proposed random sampling MPPT technique can also be implemented with parallel-connected PV

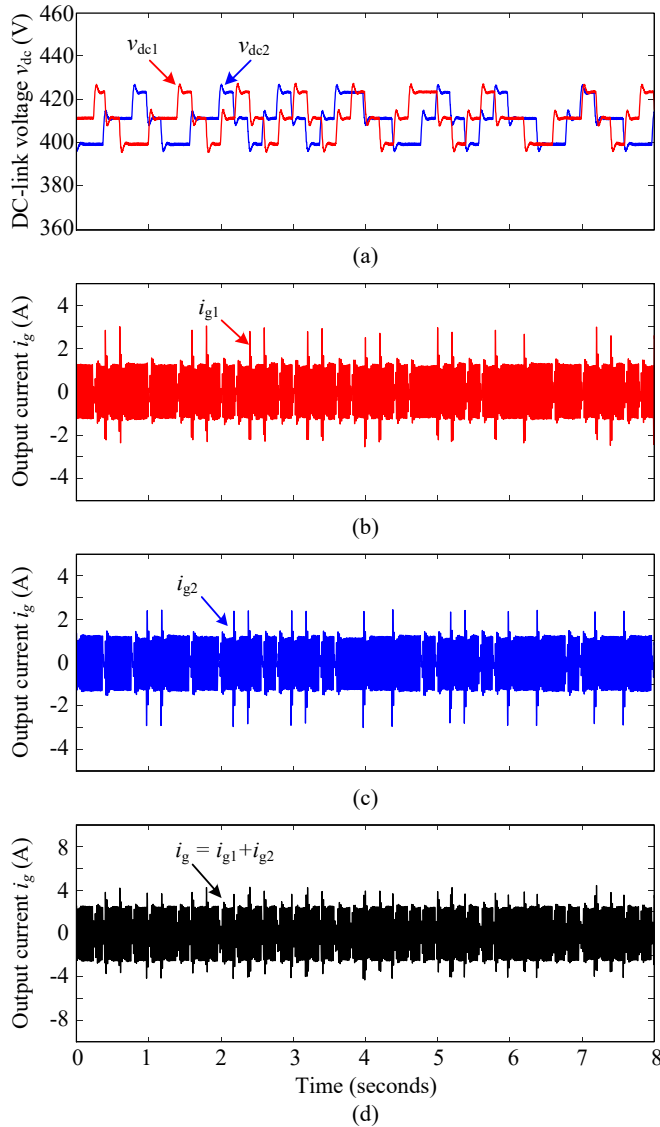


Fig. 13. Experimental waveform of the two PV inverter operated in parallel with the proposed method ($f_{\text{fast}} = 5$ Hz and $f_{\text{slow}} = 2.5$ Hz): (a) dc-link voltage of both PV strings $v_{\text{dc}1}$ and $v_{\text{dc}2}$, (b) output current of the first PV string i_{g1} , (c) output current of the second PV string i_{g2} , and (d) total output current i_g .

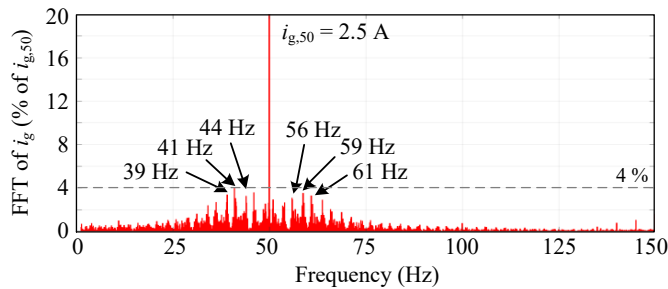


Fig. 14. Frequency spectrum of the total output current i_g of the parallel-connected PV inverter (in percentage of the 50 Hz component) with the random sampling MPPT technique.

inverters where the stochastic perturbation behavior of each PV inverter can counteract one another, resulting in an even lower interharmonics in the total output current.

ACKNOWLEDGMENT

This work was supported in part by Innovation Fund Denmark through the Advanced Power Electronic Technology and Tools (APETT) project and in part by the Reliable Power Electronic-Based Power System (REPEPS) project at the Department of Energy Technology, Aalborg University as a part of the Villum Investigator Program funded by the Villum Foundation.

REFERENCES

- [1] A. R. Oliva and J. C. Balda, "A PV dispersed generator: a power quality analysis within the IEEE 519," *IEEE Trans. Power Del.*, vol. 18, no. 2, pp. 525–530, Apr. 2003.
- [2] M. Aiello, A. Cataliotti, S. Favuzza, and G. Graditi, "Theoretical and experimental comparison of total harmonic distortion factors for the evaluation of harmonic and interharmonic pollution of grid-connected photovoltaic systems," *IEEE Trans. Power Del.*, vol. 21, no. 3, pp. 1390–1397, Jul. 2006.
- [3] A. Testa, M. F. Akram, R. Burch, G. Carpinelli, G. Chang, V. Dinavahi, C. Hatziaodoniu, W. M. Grady, E. Gunther, M. Halpin, P. Lehn, Y. Liu, R. Langella, M. Lowenstein, A. Medina, T. Ortmeier, S. Ranade, P. Ribeiro, N. Watson, J. Wikston, and W. Xu, "Interharmonics: Theory and modeling," *IEEE Trans. Power Del.*, vol. 22, no. 4, pp. 2335–2348, Oct. 2007.
- [4] T. Messo, J. Jokipii, A. Aapro, and T. Suntio, "Time and frequency-domain evidence on power quality issues caused by grid-connected three-phase photovoltaic inverters," in *Proc. EPE*, pp. 1–9, Aug. 2014.
- [5] P. Pakonen, A. Hilden, T. Suntio, and P. Verho, "Grid-connected PV power plant induced power quality problems - experimental evidence," in *Proc. EPE*, pp. 1–10, Sep. 2016.
- [6] R. Langella, A. Testa, S. Z. Djokic, J. Meyer, and M. Klatt, "On the interharmonic emission of PV inverters under different operating conditions," in *Proc. ICHQP*, pp. 733–738, Oct. 2016.
- [7] R. Langella, A. Testa, J. Meyer, F. Mller, R. Stiegler, and S. Z. Djokic, "Experimental-based evaluation of PV inverter harmonic and interharmonic distortion due to different operating conditions," *IEEE Trans. Instrum. Meas.*, vol. 65, no. 10, pp. 2221–2233, Oct. 2016.
- [8] V. Ravindran, S. K. Rnnberg, T. Busatto, and M. H. J. Bollen, "Inspection of interharmonic emissions from a grid-tied PV inverter in north Sweden," in *Proc. ICHQP*, pp. 1–6, May 2018.
- [9] N. Femia, G. Petrone, G. Spagnuolo, and M. Vitelli, "Optimization of perturb and observe maximum power point tracking method," *IEEE Trans. Power Electron.*, vol. 20, no. 4, pp. 963–973, Jul. 2005.
- [10] A. Sangwongwanich, Y. Yang, D. Sera, H. Soltani, and F. Blaabjerg, "Analysis and modeling of interharmonics from grid-connected photovoltaic systems," *IEEE Trans. Power Electron.*, vol. 33, no. 10, pp. 8353–8364, Oct. 2018.
- [11] H. Schmidt, B. Burger, U. Bussemas, and S. Elies, "How fast does an mpp tracker really need to be?" in *Proc. EU PVSEC*, pp. 3273–3276, Sep. 2009.
- [12] J. Kivimäki, S. Kolesnik, M. Sitbon, T. Suntio, and A. Kuperman, "Design guidelines for multiloop perturbative maximum power point tracking algorithms," *IEEE Trans. Power Electron.*, vol. 33, no. 2, pp. 1284–1293, Feb. 2018.
- [13] A. Sangwongwanich and F. Blaabjerg, "Mitigation of interharmonics in PV systems with maximum power point tracking modification," *IEEE Trans. Power Electron.*, vol. 34, no. 9, pp. 8279–8282, Sep. 2019.
- [14] F. Blaabjerg, J. K. Pedersen, and P. Thøgersen, "Improved modulation techniques for PWM-VSI drives," *IEEE Trans. Ind. Electron.*, vol. 44, no. 1, pp. 87–95, Feb. 1997.
- [15] S.B. Kjaer, J.K. Pedersen, and F. Blaabjerg, "A review of single-phase grid-connected inverters for photovoltaic modules," *IEEE Trans. Ind. Appl.*, vol. 41, no. 5, pp. 1292–1306, Sep. 2005.
- [16] Y. Yang and F. Blaabjerg, "Overview of single-phase grid-connected photovoltaic systems," *Electr. Power Compon. and Syst.*, vol. 43, no. 12, pp. 1352–1363, 2015.